



Molecular recognition in the sphingosine 1-phosphate receptor family

Truc-Chi T. Pham, James I. Fells Sr., Daniel A. Osborne¹,
E. Jeffrey North, Mor M. Naor, Abby L. Parrill*

Department of Chemistry and Computational Research on Materials Institute, The University of Memphis, Memphis, TN 38152, USA

Received 18 July 2007; received in revised form 1 November 2007; accepted 3 November 2007

Available online 17 November 2007

Abstract

Computational modeling and its application in ligand screening and ligand receptor interaction studies play important roles in structure-based drug design. A series of sphingosine 1-phosphate (S1P) receptor ligands with varying potencies and receptor selectivities were docked into homology models of the S1P_{1–5} receptors. These studies provided molecular insights into pharmacological trends both across the receptor family as well as at single receptors. This study identifies ligand recognition features that generalize across the S1P receptor family, features unique to the S1P₄ and S1P₅ receptors, and suggests significant structural differences of the S1P₂ receptor. Docking results reveal a previously unknown sulfur-aromatic interaction between the S1P₄ C5.44 sulfur atom and the phenyl ring of benzimidazole as well as π–π interaction between F3.33 of S1P_{1,4,5} and aromatic ligands. The findings not only confirm the importance of a cation–π interaction between W4.64 and the ammonium of S1P at S1P₄ but also predict the same interaction at S1P₅. S1P receptor models are validated for pharmacophore development including database mining and new ligand discovery and serve as tools for ligand optimization to improve potency and selectivity.

© 2007 Elsevier Inc. All rights reserved.

Keywords: Sphingosine 1-phosphate (S1P); G protein-coupled receptor (GPCR); Endothelial differentiation gene (EDG); Computational model; Ligand recognition

1. Introduction

Members of the G protein-coupled receptor (GPCR) superfamily are involved in many major diseases such as cancer, cardiovascular disease, asthma and neurodegenerative diseases, and control fundamental aspects of human physiology and behaviors [1,2]. With more than 800 unique members [3], GPCR ligands comprise over 50% of current drugs from which annual revenues exceed \$50 billion [4]. Bovine rhodopsin is the only GPCR that has been experimentally characterized at high resolution [5,6], demonstrating that three-dimensional structures for GPCR are very difficult to obtain. Knowledge about most other GPCR structures usually comes from homology models in combination with mutagenesis or pharmacological data [7]. The accuracy of these models remains unclear, but their utility in ligand screening and structure-based drug design is undeniable.

The majority of S1P receptors belong to the endothelial differentiation gene (EDG) family GPCR. Five known members of the EDG family bind S1P specifically and with affinities in the nanomolar range, including S1P₁/EDG1 [8,9], S1P₂/EDG5/H218 [10], S1P₃/EDG3 [10], S1P₄/EDG6 [11,12] and S1P₅/EDG8 [13]. S1P receptors have been discovered in almost every tissue tested, although expression levels vary significantly [14,15] indicating they have distinct functions. Cellular effects of S1P are mediated through cell-surface S1P receptors as well as uncharacterized intracellular targets. S1P is involved in angiogenesis and cell migration [16–21]. S1P action as survival factor for a variety of cell lines such as human umbilical vein endothelial cells (HUVECs) [22,23], cardiac fibroblasts [24] and oocytes [25] suggests potential therapeutic applications for S1P receptor ligands in cancer, cardiovascular disease, wound healing and inflammation. In addition, S1P and the related phosphorylated metabolite of the immune modulator FTY720 have recently been demonstrated to interfere with lymphocyte trafficking by reversibly sequestering lymphocytes in lymph nodes [26], a response which leads to immunosuppression [27]. Thus, S1P analogs and their precursors may be useful agents to protect against transplant

* Corresponding author. Tel.: +1 901 678 2638; fax: +1 901 678 3447.

E-mail address: aparrill@memphis.edu (A.L. Parrill).

¹ Current address: Department of Physiology, University of Tennessee Health Sciences Center, Memphis, TN 38163, USA.

rejection or in the treatment of autoimmune disease. One effective way of altering S1P effects is providing substances that can block or mimic its activity under pathological or biological conditions through S1P receptors.

In this study, we developed or updated models of the S1P receptor family members and computationally validated the ability of the models to reflect pharmacological trends in agonist binding. The hybrid homology models with experimentally derived loop structures better reflect ligand binding affinity at individual receptors and will be the keys for understanding the mechanism of ligand–protein interaction, identifying S1P agonists and antagonists, and evaluating lead compounds for anticancer, cardiovascular and immunosuppressive drug design.

2. Methodology

2.1. Model development

The homology model of the S1P₁ receptor was developed as described in our recent paper [28–30], and modified in the first extracellular loop (E1) based on the NMR structure of a S1P₄ E1peptidomimetic (Protein Databank [31] entry 2DCO [32]). The S1P₁ E1 structure was remodeled using MOE package [33] as follows. First, the sequence of the S1P₁ receptor was aligned against the 2DCO sequence. A homology model of S1P₁ E1, VAYTANLLLSGATTYKLTPAQWFLREGS, was generated based on 2DCO. Coordinates from A2 to E26 of the E1 model replaced corresponding residues in the S1P₁ model. The structure was minimized with the MMFF94 force field [34] at splice points (AY and EG) to a root mean square gradient (RMSG) of 1 kcal/(mol Å). The entire structure was subsequently minimized to RMSG = 0.1 kcal/(mol Å).

Homology models of the S1P₂–S1P₅ receptors were generated from the revised model of the S1P₁ receptor after sequence alignment. In addition, TM3 of S1P₃ – LREGSMF-VALGASTCSLLAIAIERHL – was remodeled as a standard helix, and then spliced into the receptor model after minimization with the MMFF94 force field [34]. For S1P₂, a single manual refinement in the agonist binding pocket was performed by rotating the ε-amine moiety of K7.34 such that the residue is positioned to interact with the phosphate functionality of S1P. All models were initially minimized to an RMSG of 1 kcal/(mol Å) while the protein backbones were fixed. The process was repeated with flexible backbones for 1000 iterations of steepest descent, followed by conjugate gradient and Truncated Newton minimizations to an RMSG of 0.1 kcal/(mol Å).

2.2. Docking studies

A series of S1P agonists (Table 1) were docked into all S1P receptor models to discover ligand binding specificity at the receptor subtype level. Phosphate and ammonium groups were assigned -2 and +1 charges, respectively. Azetidine was modeled in both *cis* and *trans* stereoisomers. All docking studies were performed with AUTODOCK version 3.0 [35]. This software allows stochastic exploration of ligand con-

formations and configurations through torsion angle rotations, molecular translations and rotations in a rigid protein. Docked complexes were rated based on energy. AUTODOCK calculates energies for various ligand atom type occupancies of grid points in a user-defined box within the protein to generate grid maps before docking ligands. The software generates grid maps for each type of atom of the ligand separately as well as an electrostatic map. Energies for various ligand poses are then computed by summing energy values from these grid maps based on the positions of each atom in the ligand. Only one set of grid maps were generated for each receptor and all studied ligands.

Default AUTODOCK parameters were used in our studies with three exceptions. The number of energy evaluations in the genetic algorithm search was increased to 9×10^{10} ; the optimization continued for 6×10^4 generations and 3000 iterations were used in the Solis and Wetts local search. A docking box of $95 \times 51 \times 51$ grid points, equivalent to $35.625 \text{ \AA} \times 19.125 \text{ \AA} \times 19.125 \text{ \AA}$, was used for all docking studies. This box contained most of the transmembrane domains and part of the extracellular loops. Docking results were analyzed based on visualized interactions and docked energy. The best conformations (lowest docked energy conformations) were minimized in the context of the fixed receptor after adding hydrogen and re-assigning charges with the MMFF force field.

3. Results

3.1. S1P receptor models

The first extracellular loop in our experimentally validated S1P₁ receptor model [28–30] was modified by analogy to the experimental NMR structure of a peptide mimetic of the first extracellular loop of S1P₄ (pdb id 2DCO) [32]. This refined S1P₁ model was used as a template for the other S1P receptor models and in docking studies with a series of ligands in order to identify the contributions to and trends in molecular recognition. Models of S1P_{2–5} receptors were developed based on the refined S1P₁ model using the sequence alignment shown in Fig. 1. S1P receptor models share similarities in helical bends and several interhelical hydrogen bond patterns. Hydrogen bonds from D2.50 to both S7.46 and N7.49 were observed for all receptor models. Meanwhile, hydrogen bonds from E1.49 to Y7.53 and from x1.59 to R7.62 as well as from N2.45 to S3.42 were detected in S1P₁, S1P₂ and S1P₄ only. A complete listing of interhelical hydrogen bonds is shown in Table 2. In comparison with bovine rhodopsin, our S1P receptor models have a shorter second extracellular loop and no disulfide bond between this loop and TM3. In addition, our models do not include an analog to helix 8 observed for bovine rhodopsin.

3.2. Binding pocket

The binding site of these receptor models consists of charged residues in TM3 (R3.28 and E3.29), TM5 (K5.38) and TM7 (R7.34) for S1P_{1–3} or W4.64 for S1P_{4–5} which interact with the

Table 1
S1P receptor agonist potencies

Structure	S1P ₁	S1P ₂	S1P ₃	S1P ₄	S1P ₅
Binding affinity (IC ₅₀ , nM) ^a					
	0.67	0.35	0.26	34	0.55
	2.3	580	3.6	140	13
Phosphonate	0.28	>10000	6.3	15	0.77
	18	>10000	4900	5400	11
Azetidine	37	>10000	>10000	>10000	4600
	20	2.2	1.2	37	1.7
Activation (EC ₅₀ , nM) ^b					
	37 (partial)	NA ^c	NA ^c	48	6.6 (partial)
Benzimidazole					

^a Data from Hale et al. [37].

^b Data from Clemens et al. [38].

^c No activation.

polar head groups of ligands. The hydrophobic tails of ligands adopt different conformations according to the geometric shape of the binding pocket. The hydrophobic tails adopt extended conformations for all ligands docked into the S1P₁ and S1P₅ receptors (Fig. 2A and B) and folded conformations in the S1P₄ receptor (Fig. 2D). This result reflects the 4 Å shorter binding pocket of S1P₄ relative to S1P₁. For the S1P₃ receptor, most of the ligands' hydrophobic tails adopted folded conformations (Fig. 2C). Fig. 3 shows the best docked complexes of selected ligands in S1P₁. As expected, docking results of S1P, FTY720P, benzimidazole, phosphonate and azetidine (Fig. 3A and B) revealed interactions between positively charged residues

R3.28, K5.38 and R7.33 and the negatively charged groups (phosphate or carboxylate) of ligands, as well as interactions between E3.29 and the ammonium nitrogen of ligands. Docking studies of SEW2871 were consistent with our docking studies using the previous S1P₁ receptor model [36]. The salt–bridge interaction of the S1P phosphate group is replaced by ion–dipole interactions involving the SEW2871 trifluoromethyl group and salt–bridge interactions of the S1P ammonium group are replaced by π-stacking interactions. In fact, the fluorine atoms of CF₃ group were 2.7–3.9 Å away from positively charged nitrogen atoms of R3.28, K5.38 and R7.34 (Fig. 3C). In addition, multiple hydrophobic residues, F3.33, W6.48 and

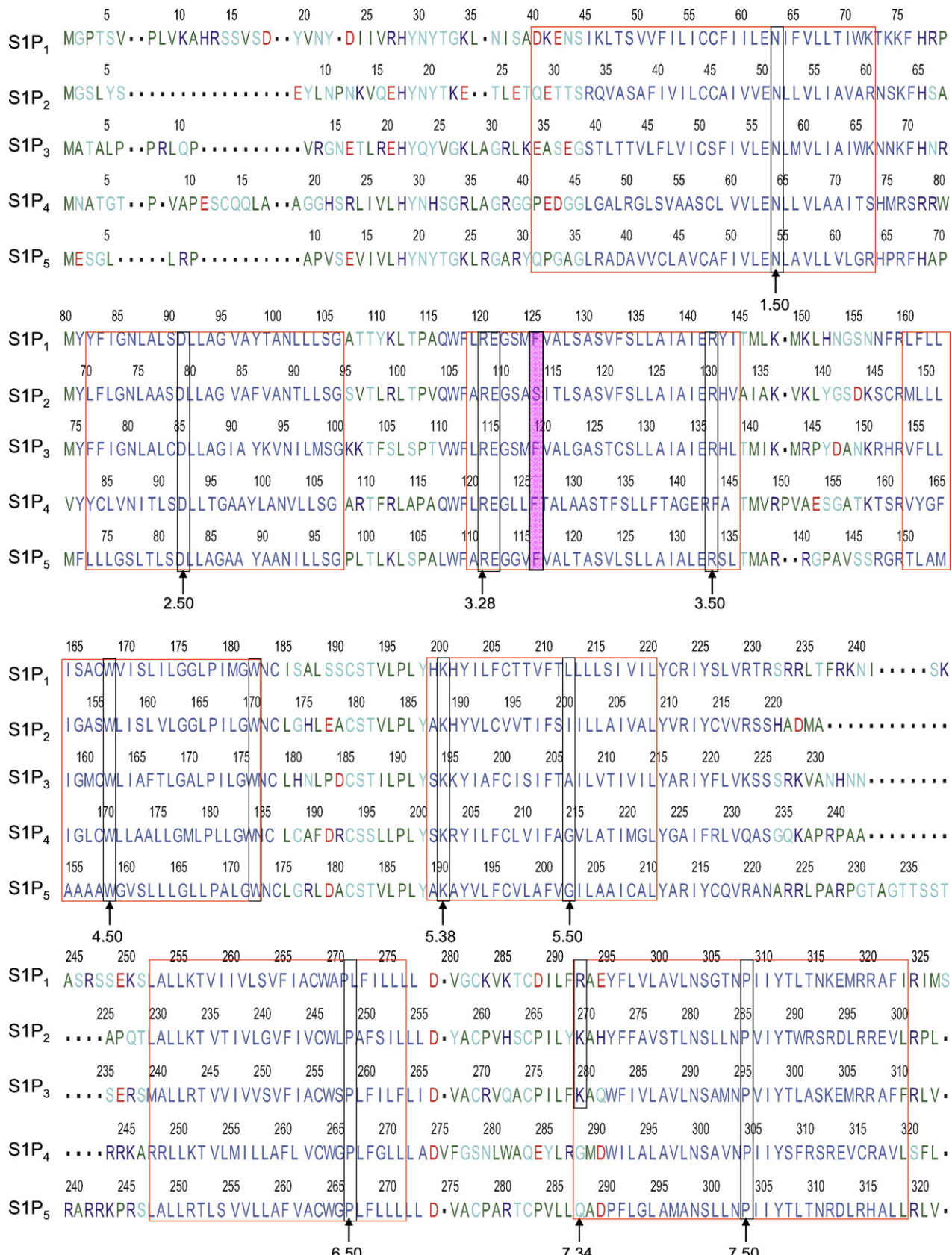


Fig. 1. Sequence alignment of S1P receptors. Red boxes indicate residues in transmembrane domains. Black boxes indicate residues at .50 as well as residues required for ligand binding and receptor activation. Purple boxes show residues required for ligand binding and receptor activation in one receptor but not others.

Table 2
Interhelical hydrogen bonding

S1P ₁	S1P ₂	S1P ₃	S1P ₄	S1P ₅
T1.35...E7.36				
E1.49...Y7.53	E1.49...Y7.53		E1.49...Y7.53	
K1.59...R7.62	R1.59...R7.62		S1.59...R7.62	
	R1.59...E7.63		S1.59...E7.59	
Y2.40...T7.54	Y2.40...T7.54			
N2.45...S3.42	N2.45...S3.42		N2.45...S3.42	
N2.45...W4.50	N2.45...W4.50			
	S2.49...A3.38			
D2.50...S7.46	D2.50...S7.46	D2.50...S7.46	D2.50...S7.46	D2.50...S7.46
D2.50...N7.49	D2.50...N7.49	D2.50...N7.49	D2.50...N7.49	D2.50...N7.49
Y2.57...E7.36				
S3.37...S4.53	S3.37...S4.53			
	F3.41...S4.49			
	R3.50...L5.58			
	H3.51...A5.57	H3.51...I5.57		
V6.43...N7.45		W6.48...F7.38	W6.48...I7.38	A6.43...N7.45

F7.38, are close in contact with the aromatic rings of SEW2871 (not shown).

3.3. S1P receptor models: reflections of ligand binding affinity

Docking results of selected ligands (Table 1) in S1P receptor models reflect the experimental trend in ligand affinity. Ligand potency has been reported for S1P₁ and S1P₄ receptors in order of FTY720P > S1P > phosphonate > azetidine > SEW2871 [37]. Docking studies indicate the numbers of complementary polar interactions within 3 Å (Table 3) are in the same order for S1P₁ and S1P₄ receptors. Additionally, the number of close complementary interactions is lower for all ligands at the S1P₄ receptor, consistent with the lower potencies observed for each agonist at this receptor. Complementary polar interactions are measured between the oxygen atoms of the carboxylate/phosphate groups of most agonists or fluorine atoms of SEW2871 to the nitrogen atoms of R3.28, K5.38 or K/R7.34, as well as between the ammonium nitrogen and the oxygen atoms of E3.29, the centroid of the five-membered ring of W4.64 and the centroid of the F3.33 phenyl ring.

Fig. 4 illustrates key interactions that explain the difference in ligand affinity for FTY720P, phosphonate and SEW2871 at the S1P₄ receptor. S1P₄ binds FTY720P through ion-pair interactions between the phosphate group and R3.28 and K5.38 as well as between the ammonium group and E2.39, and a cation–π interaction between the ammonium group and the five-membered ring of W4.64 (Fig. 4A) as observed for S1P. Interactions with the phosphonate ligand are less optimal at the ammonium group characterized by weak interactions with E3.29 (5 Å away) and negligible interaction with W4.64 (6.8 Å away) (Fig. 4B). In addition, a hydrogen bond between the hydroxyl group of FTY720P and the E3.29 oxygen atoms and a π–π interaction between the FTY720P phenyl ring and F3.33 comprise a molecular rationale for the greater potency of FTY720P at S1P₄ compared to S1P and phosphonate. Docking SEW2871 into the

S1P₄ model reveals no complementary interactions at all (Fig. 4C). This is consistent with the fact that S1P₄ has no affinity for SEW2871. For the S1P₅ receptor, the number of complementary interactions within 3 Å observed are 5, 5, 4, 3 and 2 for FTY720P, S1P, phosphonate, azetidine and SEW2871, respectively. The docking data agree with the ligand affinity trend FTY720P, S1P > phosphonate > azetidine > SEW2871 for the S1P₅ receptor [37].

Docking studies with S1P receptor models not only rationalize binding affinity of various ligands at one receptor but also binding affinities of one ligand at different S1P receptors. For example, analysis of S1P docking results indicates the number of strong interactions characterized by distances less than 3 Å between the S1P head group and complementary sites in S1P_{1–5} are 5, 6, 7, 4 and 5, respectively. This result is consistent with affinities reported for S1P across the receptor family: S1P₃ > S1P₂ > S1P₅ ~ S1P₁ > S1P₄.

3.4. Strengths/weaknesses of the S1P₂ receptor model

Although docking S1P and SEW2871 into the S1P₂ model resulted in good agreement with other receptor models and experimental trends, data on other ligands failed to reflect relative binding affinities. Binding assays carried out by Hale et al. [37] show S1P₂ does not bind FTY720P, phosphonate and azetidine. In contrast to experimental studies, docking results with the S1P₂ receptor model indicated this receptor interacts favorably with all studied ligands, except SEW2871 (Fig. 5A). The greatest inconsistency between the model and experimental observation is observed for phosphonate. The ammonium group of phosphonate interacts weakly with E3.29 of the S1P₁ (Fig. 5B) and S1P_{3–5} receptors. The distance from the ammonium nitrogen atom to the E3.29 oxygen atom is about 4.7–5.0 Å. Meanwhile the corresponding distance observed for S1P₂ receptor is 2.4 Å (Fig. 5C). Due to inconsistent docking results on this receptor, we are in the process of experimentally characterizing the binding pocket to refine the model.

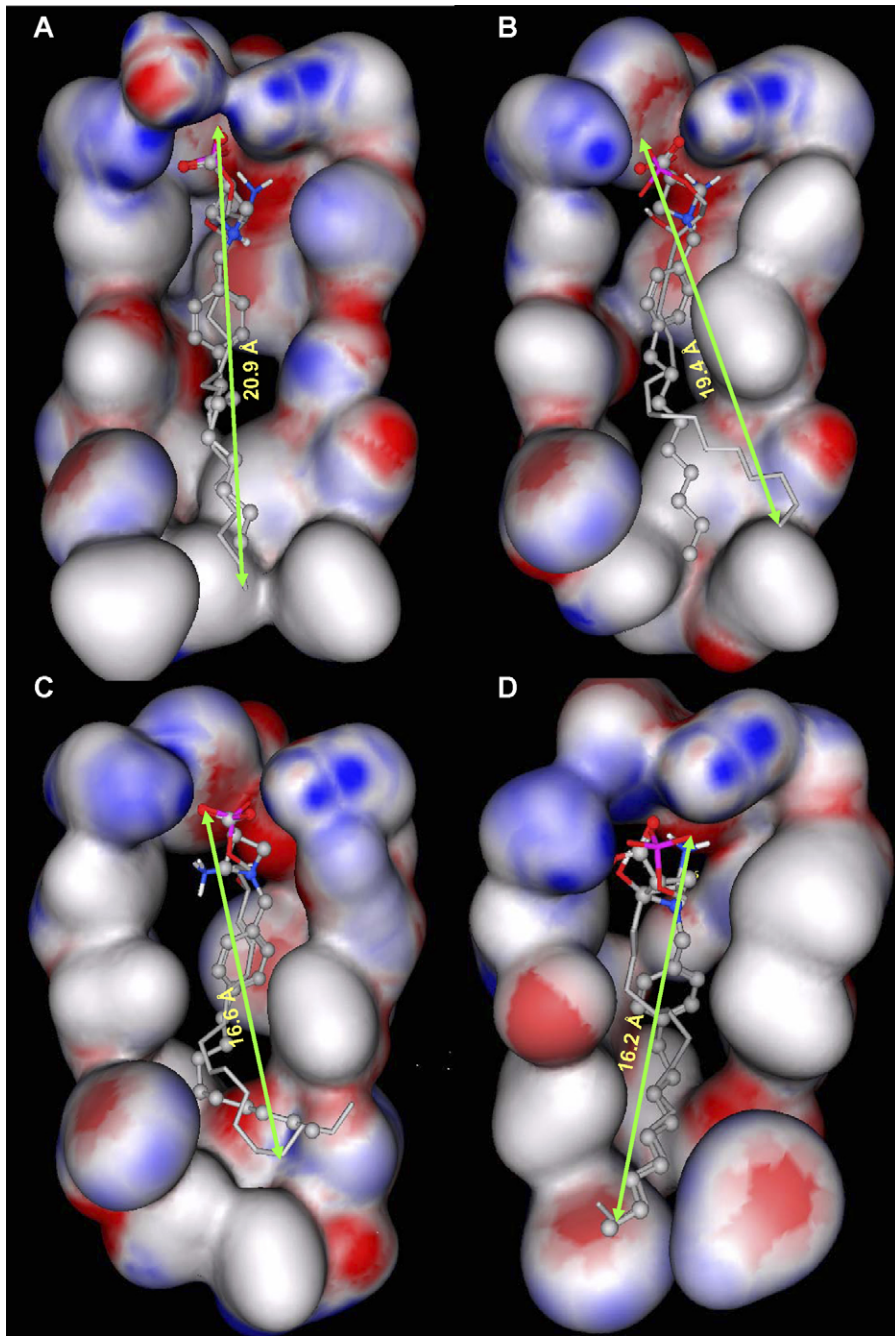


Fig. 2. Electrostatic surfaces of S1P receptor binding pockets. Gauss Connolly surfaces colored by atomic partial charge (red indicates negative, white indicates neutral and blue indicates positive partial charge) for atoms within 4.5 Å of S1P in TM3-5 were computed with the MOE program. The bound position of S1P is shown as a stick model and azetidine as stick and ball model. S1P₁ binding pocket with docked position of S1P (A) is more than 4 Å longer than S1P₃ binding pocket with docked position of S1P (C) and S1P₄ binding pocket with docked position of S1P (D), and 1 Å longer than S1P₅ binding pocket with docked position of S1P (B).

3.5. Ligand recognition differences among the S1P receptor family

Docking studies with S1P receptor models revealed significant differences in ligand recognition among this family, especially for benzimidazole. Benzimidazole activates 3 out of 5 S1P receptors and fully agonizes only the S1P₄ receptor [38]. Docking results show that the benzimidazole headgroup

interactions with S1P₁, S1P₄ and S1P₅ are similar to those of S1P. More favorable cation–π and π–π interactions involving the benzimidazole ammonium nitrogen and five-membered ring, respectively, and F3.33 phenyl ring (Fig. 6A and B) may account for the activation response at S1P₁, S1P₄ and S1P₅ receptors but not S1P₂ and S1P₃ receptors. Table 4 presents the measured distances for these interactions and those involving the sulfur atom of C5.44. Interestingly, the distance

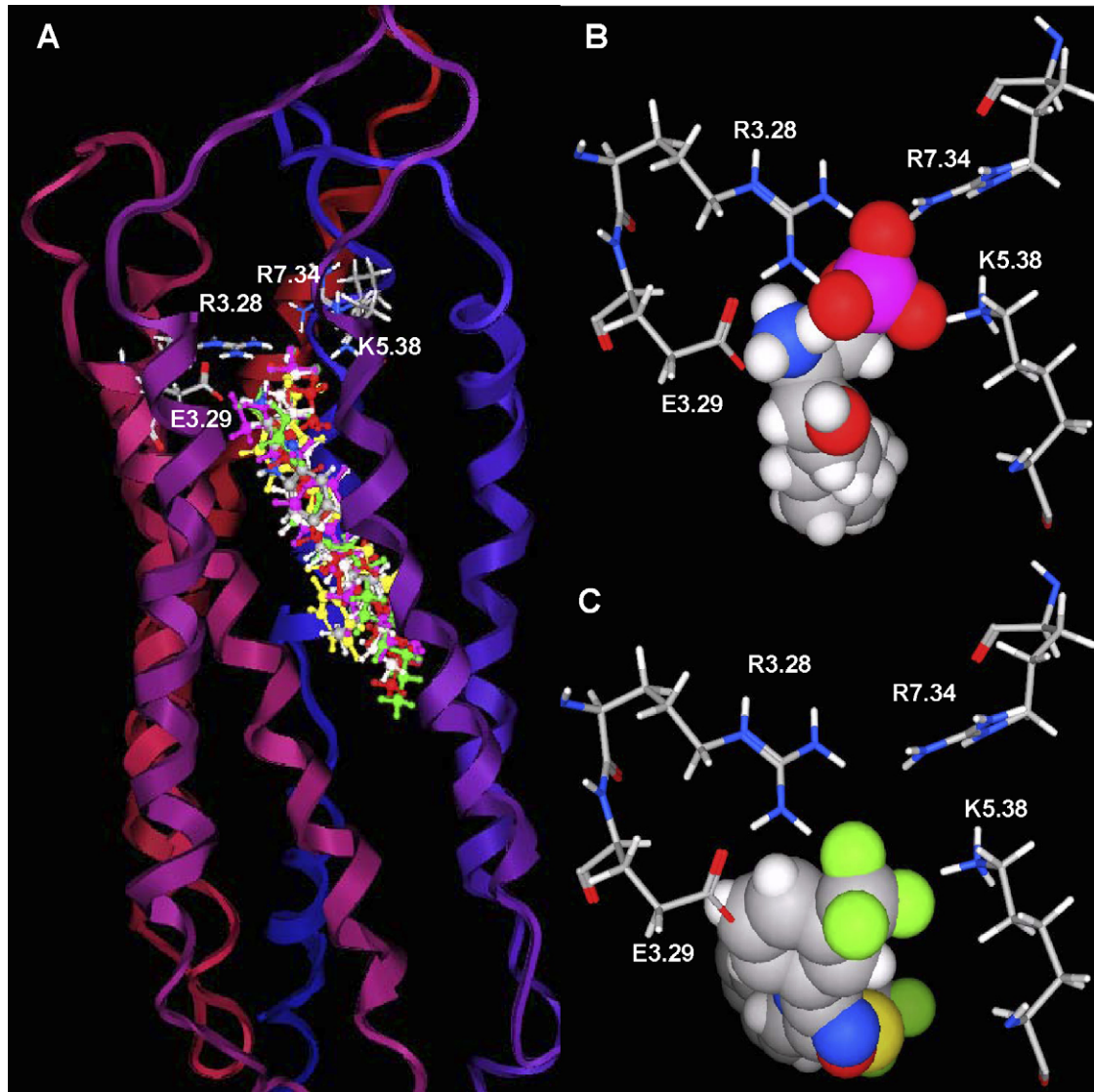


Fig. 3. Refined S1P₁ receptor model. Panel A. S1P₁ complex with FTY720P, S1P, benzimidazole, phosphonate, azetidine and SEW2871. The model is shown with extracellular loops at the top. Ribbons colored from red at the amino terminus to blue at the carboxy terminus represent the backbone of S1P₁. The stick atoms represent residues required for ligand binding (red: oxygen, blue: nitrogen, grey: carbon, white: hydrogen and magenta: phosphorus). The ball & stick atoms represent ligands; FTY720P (magenta), S1P (green), benzimidazole (element), phosphonate (red), azetidine (light grey) and SEW2871 (yellow). Panel B. View of the S1P₁ complex with S1P from the extracellular space. Selected residues are shown as stick models and labeled. Panel C. View of the S1P₁ complex with SEW2871 from the extracellular space. Selected residues are shown as stick models and labeled.

Table 3

Number of interactions within 3 Å between the polar head groups of ligands and N/O atoms of charged residues in TM 3, 5 and 7

Ligand/receptor	S1P ₁	S1P ₂	S1P ₃	S1P ₄	S1P ₅
FTY720P	7	5	7	6	5
S1P	5	6	7	4	5
Benzimidazole	5	7	7	4	4
Phosphonate	4	6	6	3	4
Azetidine(<i>cis</i>)	3	4	5	2	3
Azetidine(<i>trans</i>)	3	4	5	2	3
SEW2871	2	0	0	0	2

between C5.44-S of S1P₄ and the six-membered ring of benzimidazole ($D = 5.4 \text{ \AA}$) is unique across the receptor family in meeting the criterion for favorable interaction ($D \leq 6 \text{ \AA}$) [39]. This ligand–protein recognition feature distinguishes S1P₄ from other members of S1P receptor family.

Ligand recognition differences were also detected for S1P. S1P is the endogenous ligand for the S1P receptors, but only a subset of the complementary interaction sites are conserved across the entire receptor family. Docking studies revealed a cation–π interaction between the ammonium group of S1P and the W4.64 pyrrole ring in the S1P₄ and S1P₅ receptors with distances of 4.9 (Fig. 6C) and 4.4 Å. The corresponding

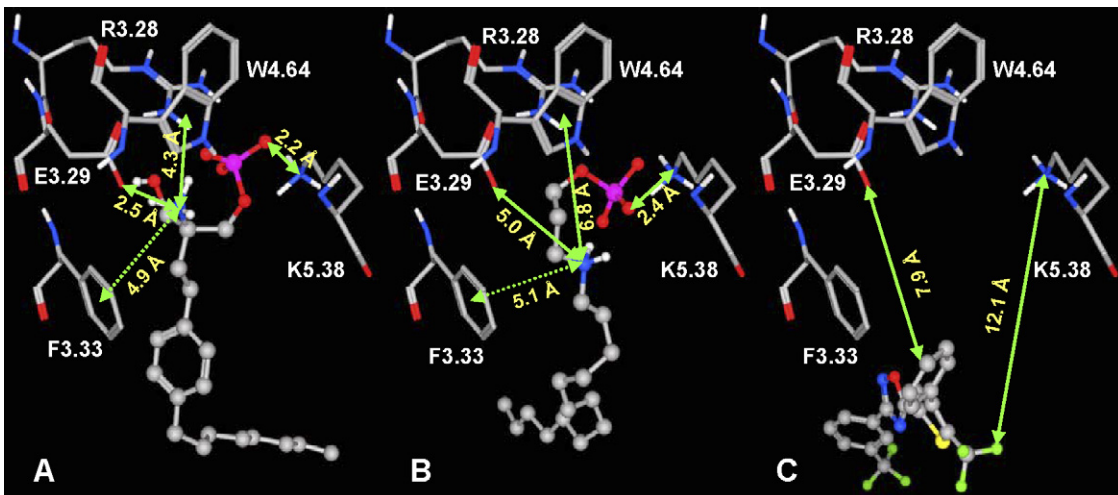


Fig. 4. Interaction vs. ligand binding affinity at S1P₄. S1P₄ complex with FTY720P (A), phosphonate (B) and SEW2871 (C). Ball and stick atoms represent ligands and stick atoms represent residues required for ligand binding. Non-polar hydrogens are omitted for clarity. S1P₄ interactions with ligands in order FTY720P (A) > S1P ~ benzimidazole > phosphonate (B) > Azetidine > SEW2871 (C) agree with binding affinity observed for these ligands (Table 1).

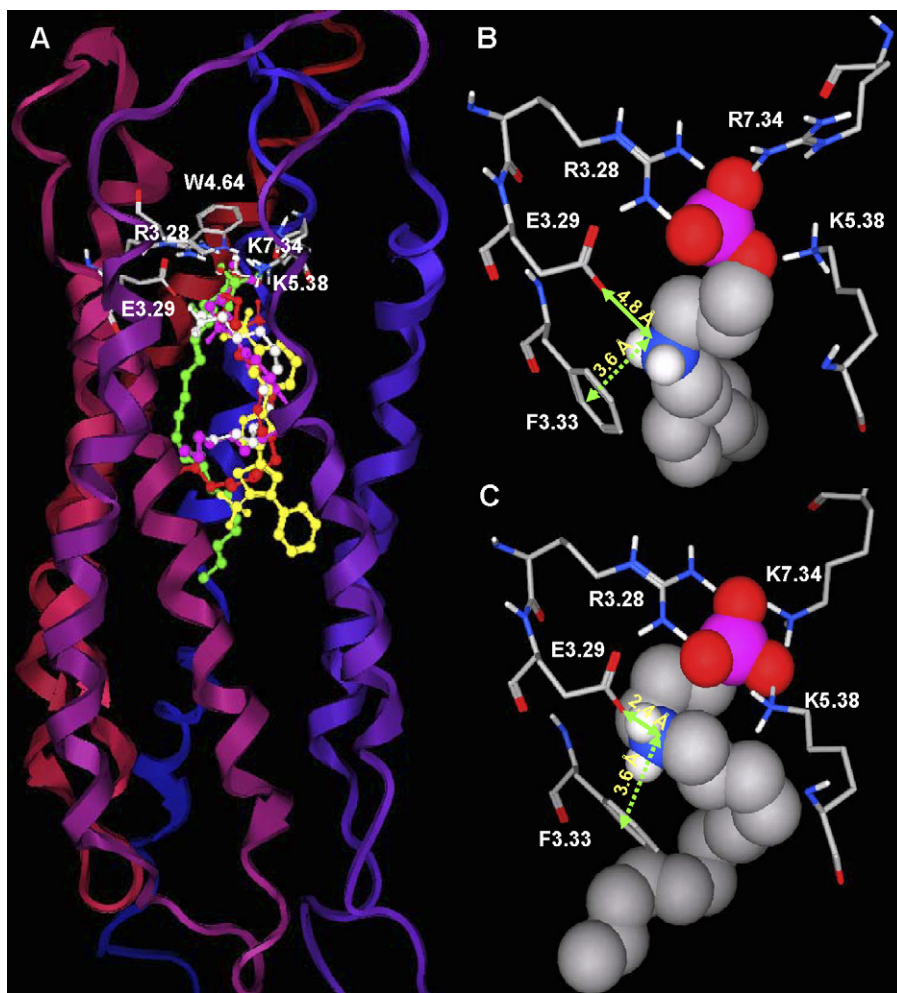


Fig. 5. Failure of S1P₂ homology model to reflect pharmacological trend. Panel A. A homology model of S1P₂ receptor was generated using the refined S1P₁ model. S1P₂ complexes with S1P, phosphonate and SEW2871 are colored as described for Fig. 3A. Panels B and C illustrate the failure of S1P₂ model to accurately reflect the pharmacological trend based on the distances between the ammonium group of phosphonate and E3.29 and F3.33 aromatic centroid for S1P₁ (B) and S1P₂ (C). Residues required for ligand binding are shown in stick with non-polar hydrogens omitted for clarity. Phosphonate is shown in space filling atoms. The models suggest stronger phosphonate interactions with S1P₂ (shorter distances) than S1P₁ (longer distances) which is contrary to the fact that S1P₂ has no affinity to phosphonate.

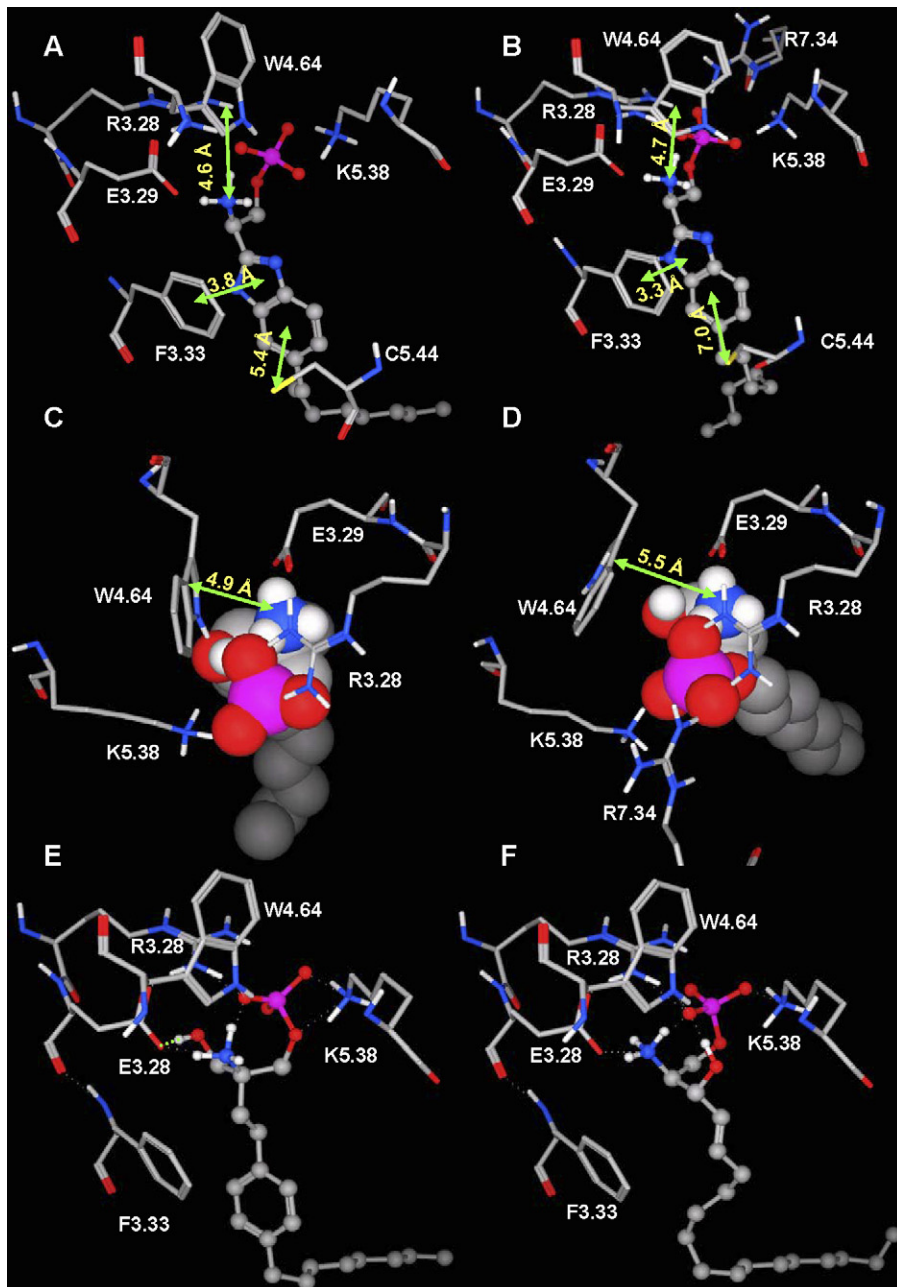


Fig. 6. Ligand recognition differences in the S1P receptor family. Panels A and B. Benzimidazole interacts selectively with C5.44 of S1P₄ (A) but not S1P₁ (B). The S1P₄ C5.44 sulfur atom is closer to the optimized position for sulfur–aromatic interaction (5.4 Å); while the S1P₁ C5.44 sulfur atom more distant from the imidazole ring (7.0 Å). Views and labels are similar to Fig. 5. Panels C and D. S1P (space filling atoms) interacts selectively with W4.64 of S1P₄ (C) but S1P₁ (D). The distance between ammonium nitrogen and W4.64 pyrrolic centroid is <5 Å for S1P₄ and >5 Å for S1P₁. Views are the same for C and D but different from A and B. Panels E and F. FTY720P (E) and S1P (F) recognize the S1P₄ receptor differently. The hydroxyl group of FTY720P forms a hydrogen bond with the E3.29 oxygen atom (E). This extra interaction explains the higher binding affinity of FTY720P compared to S1P.

distances in S1P_{1–3} are 5.5 (Fig. 6D), 7.9 and 6.7 Å, respectively, suggesting a minimal contribution to overall S1P binding affinity at these receptors. In addition, the hydroxyl group of S1P is probably involved in ligand recognition only at S1P₃. In contrast to S1P, the hydroxyl group of FTY720P is involved in ligand binding observed for all receptor models. This feature may contribute to higher affinity of FTY720P compared to S1P (Fig. 6E and F).

4. Discussion

Our S1P receptor models define important features of ligand recognition in this family and provide a molecular rationale for the trends in ligand binding affinity for a series of ligands at a single receptor and for a single ligand across the receptor family. The general trend observed experimentally for binding affinity is in order of FTY720P,

Table 4

Observed distances (\AA) between ammonium nitrogen (N) atom or centroid of five-membered ring (5R)/phenyl ring (6R) of benzimidazole and F3.33-6R, W4.64-5R or C5.44 sulfur atom (S)

Ligand/receptor site	S1P ₁	S1P ₂	S1P ₃	S1P ₄	S1P ₅
N...W4.64-5R	4.7	4.6	5.4	4.6	5.0
N...F3.33-6R	4.9	4.8	5.1	4.9	4.9
5R...F3.33-6R	3.3	4.7	5.0	3.8	4.2
6R...C5.44-S	7.0	10.7 ^a	9.5	5.4	7.6

^a Distance between the centroid of phenyl ring of benzimidazole and C5.43-S instead of C5.44-S.

S1P > phosphonate > azetidine > SEW2871, except S1P₃ [37]. Our docking studies indicated ligands with phosphate (−2 charge) head groups (FTY720P and S1P) have stronger ion-pair interactions with positively charged residues in TM3, 5 and 7 than ligands containing carboxylate (−1 charge) head groups (azetidine *cis* and *trans*) (Table 3). The phosphonate ligand interacts somewhat between the previous two functional groups. SEW2871 lacks an anionic head group and exhibits the weakest interaction (Table 3). Among dianionic head groups, interactions are in the order of FTY720P \geq S1P > phosphonate (Table 3), except at S1P₂ and S1P₃. The S1P₃ receptor has higher affinity to S1P than FTY720P. Docking results indicate S1P₃ is the only receptor with a specific hydrogen-bonding interaction with the S1P hydroxyl group. The average distance from the S1P hydroxyl hydrogen atom to S1P₃ E3.29 oxygen atoms is 2.4 \AA . In addition, the S1P C4 = C5 double bond is located near the S1P₃ F3.33 phenyl ring (<4 \AA), suggesting possible π – π interaction. Previous studies on S1P stereoisomers and analogs examined the difference between C3 hydroxyl, C3 oxo, and C3 dehydroxy compounds [40,41]. The C3 dehydroxy findings are not particularly useful for direct comparison to our docking results as the dehydroxy compound was saturated, and two carbons shorter than S1P. However, the binding data on these compounds suggested that the C3 hydroxyl group has some effect on ligand binding at S1P_{1,3,5}. Removal of this functional group while concurrently saturating C4-C5 and reducing the carbon chain length by two atoms results in reducing binding affinity compared to S1P approximately 18 and 16% for S1P₃ and S1P₅. With other S1P receptors, FTY720P interacts more strongly than S1P due to an extra hydrogen-bonding interaction between the FTY720P hydroxyl group and the E3.29 oxygen atom (Fig. 6). Meanwhile, the phosphonate ligand has much weaker ion-pair interaction between the phosphonate ammonium group and E3.29 (Fig. 4).

A case study of benzimidazole revealed interesting observations on ligand binding with potential impact on receptor activation. Our docking results support a π – π interaction between the aromatic rings of benzimidazole and F3.33 as well as weak cation– π interactions between the ammonium nitrogen and aromatic rings of W4.64 and F3.33 of S1P₁, S1P₄ and S1P₅ (Table 4) that likely contribute to receptor activation of S1P₁, S1P₄ and S1P₅. Considerably weaker interactions of these functional groups are observed for S1P₂

and S1P₃ receptors (Table 4, observed distances [D] \sim 5 \AA). Moreover, an additional sulfur–aromatic interaction was observed only in the S1P₄ receptor. The distance from the C5.44 sulfur atom to the centroid of the benzimidazole phenyl ring is 5.4 \AA , only 0.1 \AA longer than the optimized distance for sulfur–aromatic interactions in proteins [39]. The corresponding distances observed for other receptors are at least 7 \AA , indicating negligible interaction between the functional groups (favorable interaction requires D \leq 6 \AA). This distinct interaction is expected to be a key contribution to the full agonism of benzimidazole at the S1P₄ receptor.

C5.44 is present in 4 out of 5 S1P receptors. S1P₂ has cysteine at position 5.43 instead of 5.44. With the exception of S1P₄, those cysteine sulfur atoms are at least 7 \AA away from the aromatic rings of FTY720P, benzimidazole, azetidine and SEW2871 and, therefore, may not be involved in ligand binding at S1P_{1,2,3,5} receptors. In contrast, the S1P₄ C5.44 sulfur is in the range of interaction with the aromatic rings of FTY720P, benzimidazole and azetidine. This sulfur–aromatic interaction is unique feature of S1P₄ receptor, probably arising due to the folded shape of the binding pocket (Fig. 2D).

Our previous studies [28,29,42] and current S1P receptor models indicate that the binding pocket of S1P₄ (Fig. 2D) is shorter than that of S1P₁ (Fig. 2A). S1P₁ prefers a linear binding mode and has a higher affinity to unsaturated ligands while S1P₄ prefers a bent binding mode and saturated ligands [28,29,42]. Docking results show the hydrophobic tails of all studied ligands are extended when docked into S1P₁ and S1P₅ models, but folded in the S1P₄ binding pocket. Differences in binding modes and geometry of the binding pockets lead to differential binding across the S1P receptors. For example, S1P₄ has much lower binding affinities to azetidine, approximately 300–500-fold compared to S1P₁ and S1P₅. This may be due to a combined effect of shorter binding pocket and bent binding mode required for S1P₄ [28]. The distance between negatively and positively charged groups of azetidine is one atom less than phosphate ligands. In addition, the nitrogen atom of azetidine is involved in the ring system. Both factors prevent azetidine from adopting an optimized conformation for the bent binding mode that results in lower binding affinity of azetidine at S1P₄. S1P₃ has similar binding affinity to azetidine as S1P₄ [37] and, therefore, is expected to interact with azetidine similarly to S1P₄. In fact, docked conformations of azetidine at both S1P₃ and S1P₄ have a comparable length about 3 \AA shorter than those at S1P₁ and S1P₅. Moreover, S1P₃ and S1P₄ have analogous electrostatic distributions at the top of the binding pockets with anionic charge concentrated in a small area (Fig. 2C and D) that prevents them from effectively interacting with the nitrogen atom in the ring system. In contrast, negative charge on the top of the S1P₁ and S1P₅ binding pockets distributes into an extended surface (Fig. 2A and B) allowing these receptors to interact with the azetidine nitrogen atom more effectively than S1P₃ and S1P₄.

It is known that S1P head groups bind S1P receptors via ion-pair interactions with residues R3.28, E3.29, K5.38 and R/K7.33 [28–30]. S1P₄ and S1P₅ receptors lack the positively

charged residue in TM7. Instead, S1P₄ interacts with S1P through an extra cation–π interaction between the W4.64 pyrrole ring and the ammonium group of S1P (Fig. 6). A similar result was observed for the S1P–S1P₅ complex, but not the S1P–S1P₁ (Fig. 6), S1P–S1P₂ or S1P–S1P₃ complexes. Previous model-driven mutagenesis studies of S1P receptors showed that W4.64 is required for S1P binding to the S1P₄ receptor, but not to S1P₁ [28]. Our docking studies suggest that a cation–π interaction with W4.64 is also required for S1P binding to the S1P₅ receptor to compensate for the lack of a positively charged residue in TM7, and is not necessary for S1P binding to the S1P₂ and S1P₃ receptors.

Docking studies of SEW2871 into S1P₁ receptor models reveal significant interactions with S1P₁ that overlap those of S1P. The results suggest ion–dipole interactions between the CF₃ group attached on ring A of SEW2871 and R3.28, E3.29, K5.38 and R7.34 residues that support ion-pair interactions with S1P polar head groups. In addition, multiple hydrophobic interactions between residues F3.33, W6.48 and F7.38 and the aromatic rings of SEW2871 probably contribute to SEW2871 potency at S1P₁. Our previous studies on this agonist indicate that mutation of any of R3.28, E3.29 and R7.34 residues to alanine severely reduced the phosphorylation of both Akt and ERK2 by both S1P and SEW2871 [36]. SEW2871 has been shown to be a full agonist of S1P₁ [43]. Its binding affinity at S1P₁ is about 50-fold less than S1P [37] implying that the strength of dipole–ion interactions is not adequate to replace salt bridge interactions. However, these interactions certainly contribute to the potency of SEW2871 at the S1P₁ receptor. Replacement of the CF₃ group on ring D with a methyl group significantly diminishes Akt and ERK2 responses in the E3.29A and R7.34A mutants [36] confirming an important role for this functional group.

Several models of S1P receptors have been published in the literature by at least four different research groups [41,44,45]. Models generated from the TASSER program [45] have similar overall folding as ours. However, in the TASSER models, the sidechains of R3.28, E3.29, K5.38 and R/K7.33 point away from the binding pockets. Our published mutagenesis studies indicate these residues are necessary for ligand binding and receptor activation [28,30]. A model of S1P₁ developed by Lim et al. [41] includes ion-pairing interactions between the S1P phosphate and R3.28, R7.34 as well as an ionic interaction between the S1P ammonium group and E3.29 analogous to our model. This group suggests hydrogen bonds from the Y2.57 (98) sidechain hydroxyl group and the F7.38 (296) backbone carbonyl group to the S1P hydroxyl group, which are not observed in our studies. A model of human S1P₄ has been reported in the literature that differs from our current human S1P₄ and previously published mouse [28] and human [42] S1P₄ models. Vaidehi et al. [44] indicated S1P interacts with human S1P₄ at residues T3.34(127), E7.30(284) and W7.37(291). All these residues are located toward the extracellular loops in our model, and; therefore, are unlikely interact with S1P. In addition, the hydrophobic region of the ligand binding pocket of our S1P₁ model has been experimentally validated [29].

5. Conclusions

This study identifies ligand recognition features that generalize across the S1P receptor family as well as features unique to the S1P₄ and S1P₅ receptors. Docking results highlight the previously unknown sulfur–aromatic interaction between the S1P₄ C5.44 sulfur atom and the phenyl ring of benzimidazole as well as π–π interactions between F3.33 and ligand aromatic rings. The findings not only confirm the importance of cation–π interaction between W4.64 and the ammonium of S1P at S1P₄ but also predict the same interaction at S1P₅. These docking studies provide molecular insights into pharmacological trends both across the receptor family as well as at single receptors.

Consistency with pharmacological trends qualitatively validates the S1P₁ and S1P_{3–5} models for pharmacophore development including database mining and new ligand discovery. The S1P₁ model, in fact, has already identified experimentally confirmed hits on the basis of partial matches to an agonist pharmacophore [29]. These models can also serve as tools for ligand optimization to improve potency and selectivity. For quantitative applications, such as free energy perturbation or thermodynamic integration, quantum mechanical studies and mutagenesis have validated the quantitative accuracy of the headgroup binding site [46] additional evaluations are necessary to validate the quantitative accuracy of the models.

Note added in proof

Crystallographic structures of a second GPCR, the beta2-adrenergic receptor, have been recently reported (Cherezov et al., 2007; Rosenbaum et al., 2007; Rasmussen et al., 2007).

Acknowledgments

This work was supported in part by grants from NIH-NHLBI and NIH-NCI (R01 HL084007 and R01 CA92160). We acknowledge the Chemical Computing Group for generously donating the MOE program.

References

- [1] A.M. Spiegel, L.S. Weinstein, Inherited diseases involving G proteins and G protein-coupled receptors, *Ann. Rev. Med.* 55 (2004) 27–39.
- [2] T. Schoneberg, A. Schulz, H. Biebermann, T. Hermsdorf, H. Rompler, K. Sangkuhl, Mutant G-protein-coupled receptors as a cause of human diseases, *Pharmacol. Ther.* 104 (2004) 173–206.
- [3] K.L. Pierce, R.T. Premont, R.J. Lefkowitz, Seven-transmembrane receptors, *Nat. Rev. Mol. Cell. Biol.* 3 (2002) 639–650.
- [4] M.A.N. Staff, World's best-selling medicines, *Med. Ad. News.* 23 (2004) 60–64.
- [5] K. Palczewski, T. Kumasaka, T. Hori, C.A. Behnke, H. Motoshima, B.A. Fox, I. Le Trong, D.C. Teller, T. Okada, R. Stenkamp, M. Yamamoto, M. Miyano, Crystal structure of rhodopsin: A G protein-coupled receptor, *Science* 289 (2000) 739–745.
- [6] T. Okada, M. Sugihara, A.N. Bondar, M. Elstner, P. Entel, V. Buss, The retinal conformation and its environment in rhodopsin in light of a new 2, 2 A crystal structure, *J. Mol. Biol.* 342 (2004) 571–583.

- [7] O.M. Becker, S. Shacham, Y. Marantz, S. Noiman, Modeling the 3D structure of GPCRs: advances and application to drug discovery, *Curr. Opin. Drug Discov. Dev.* 6 (2003) 353–361.
- [8] H. Okamoto, N. Takuwa, K. Gonda, H. Okazaki, K. Chang, Y. Yatomi, H. Shigematsu, Y. Takuwa, EDG1 is a functional sphingosine-1-phosphate receptor that is linked via a $G_{i/o}$ to multiple signaling pathways, including phospholipase C activation, Ca^{2+} mobilization, Ras-mitogen-activated protein kinase activation, and adenylyl cyclase inhibition, *J. Biol. Chem.* 273 (1998) 27104–27110.
- [9] M.-J. Lee, J.R. Van Brocklyn, S. Thangada, C.H. Liu, A.R. Hand, R. Menzleev, S. Spiegel, T. Hla, Sphingosine-1-phosphate as a ligand for the G protein-coupled receptor EDG-1, *Science* 279 (1998) 1552–1555.
- [10] S. An, T. Bleu, W. Huang, O.G. Hallmark, S.R. Coughlin, E.J. Goetzl, Identification of cDNAs encoding two G protein-coupled receptors for lysosphingolipids, *FEBS Lett.* 417 (1997) 279–282.
- [11] J.R. Van Brocklyn, M.H. Gräler, G. Bernhardt, J.P. Hobson, S. Spiegel, Sphingosine-1-phosphate is a ligand for the G protein-coupled receptor EDG-6, *Blood* 95 (2000) 2624–2629.
- [12] Y. Yamazaki, J. Kon, K. Sato, H. Tomura, M. Sato, T. Yoneya, H. Okazaki, F. Okajima, H. Ohta, Edg-6 as a putative sphingosine 1-phosphate receptor coupling to $Ca(2+)$ signaling pathway, *Biochem. Biophys. Res. Commun.* 268 (2000) 583–589.
- [13] D.-S. Im, C.E. Heise, N. Ancellin, B.F. O'Dowd, G.-J. Shei, R.P. Heavens, M.R. Rigby, T. Hla, S. Mandala, G. McAllister, S.R. George, K.R. Lynch, Characterization of a novel sphingosine 1-phosphate receptor, Edg-8, *J. Biol. Chem.* 275 (2000) 14281–14286.
- [14] A.J. MacLennan, C.S. Browe, A.A. Gaskin, D.C. Lado, G. Shaw, Cloning and characterization of a putative G-protein coupled receptor potentially involved in development, *Mol. Cell. Neurosci.* 5 (1994) 201–209.
- [15] T. Hla, T. Maciag, An abundant transcript induced in differentiating human endothelial cells encodes a polypeptide with structural similarities to G-protein-coupled receptors, *J. Biol. Chem.* 265 (1990) 9308–9313.
- [16] F. Wang, J.R. Van Brocklyn, J.P. Hobson, S. Movafagh, Z. Zukowska-Grojec, S. Milstien, S. Spiegel, Sphingosine 1-phosphate stimulates cell migration through a G_i -coupled cell surface receptor A potential involvement in angiogenesis, *J. Biol. Chem.* 274 (1999) 35343–35350.
- [17] E. Kupperman, S. An, N. Osborne, S. Waldron, D.Y.R. Stainier, A sphingosine-1-phosphate receptor regulates cell migration during vertebrate heart development, *Nature* 406 (2000) 192–195.
- [18] D. English, J.G. Garcia, D.N. Brindley, Platelet-released phospholipids link haemostasis and angiogenesis, *Cardiovasc. Res.* 49 (2001) 588–599.
- [19] W. Erl, W. Siess, Sphingosine-1-phosphate and the leading edg-1 of vascular smooth muscle cells, *Circ. Res.* 89 (2001) 474–476.
- [20] H.M. Rosenfeldt, J.P. Hobson, M. Macyka, A. Olivera, V.E. Nava, S. Milstien, S. Spiegel, EDG-1 links the PDGF receptor to Src and focal adhesion kinase activation leading to lamellipodia formation and cell migration, *FASEB J.* 15 (2001) 2649–2659.
- [21] K. Tamama, J. Kon, K. Sato, H. Tomura, A. Kuwabara, T. Kimura, T. Kanda, H. Ohta, M. Ui, I. Kobayashi, F. Okajima, Extracellular mechanism through the Edg family of receptors might be responsible for sphingosine-1-phosphate-induced regulation of DNA synthesis and migration of rat aortic smooth-muscle cells, *Biochem. J.* 353 (2001) 139–146.
- [22] Y.G. Kwon, J.K. Min, K.M. Kim, D.J. Billiar, Y.M. Kim, Sphingosine 1-phosphate protects human umbilical vein endothelial cells from serum-deprived apoptosis by nitric oxide production, *J. Biol. Chem.* 276 (2001) 10627–10633.
- [23] N. Hisano, Y. Yatomi, K. Satoh, S. Akimoto, M. Mitsumata, M.A. Fujino, Y. Ozaki, Induction and suppression of endothelial cell apoptosis by sphingolipids: a possible in vitro model for cell-cell interactions between platelets and endothelial cells, *Blood* 93 (1999) 4293–4299.
- [24] L. Cavallini, R. Venerando, G. Miotti, A. Alexandre, Ganglioside GM1 protection from apoptosis of rat heart fibroblasts, *Arch. Biochem. Biophys.* 370 (1999) 156–162.
- [25] Y. Morita, G.I. Perez, F. Paris, S.R. Miranda, D. Ehleiter, A. Haimovitz-Friedman, Z. Fuks, Z. Xie, J.C. Reed, E.H. Schuchman, R.N. Kolesnick, J.L. Tilly, Oocyte apoptosis is suppressed by disruption of the *acid sphingomyelinase* gene or by sphingosine-1-phosphate therapy, *Nat. Med.* 6 (2000) 1109–1114.
- [26] S. Mandala, R. Hajdu, J. Bergstrom, E. Quackenbush, J. Xie, J. Milligan, R. Thornton, G.J. Shei, D. Card, C. Keohane, M. Rosenbach, J. Hale, C.L. Lynch, K. Rupprecht, W. Parsons, H. Rosen, Alteration of lymphocyte trafficking by sphingosine-1-phosphate receptor agonists, *Science* 296 (2002) 346–349.
- [27] V. Brinkmann, D.D. Pinschewer, L. Feng, S. Chen, FTY720: altered lymphocyte traffic results in allograft protection, *Transplantation* 72 (2001) 764–769.
- [28] Y. Inagaki, T.T. Pham, Y. Fujiwara, T. Kohno, D.A. Osborne, Y. Igarashi, G. Tigyi, A.L. Parrill, Sphingosine 1-phosphate analogue recognition and selectivity at $S1P_4$ within the endothelial differentiation gene family of receptors, *Biochem. J.* 389 (2005) 187–195.
- [29] Y. Fujiwara, D.A. Osborne, M.D. Walker, D.A. Wang, D.A. Bautista, K. Liliom, J.R. Van Brocklyn, A.L. Parrill, G. Tigyi, Identification of the hydrophobic ligand binding pocket of the $S1P_1$ receptor, *J. Biol. Chem.* 282 (2007) 2374–2385.
- [30] D.A. Wang, Z. Lorincz, D.L. Bautista, K. Liliom, G. Tigyi, A.L. Parrill, A single amino acid determines lysophospholipid specificity of the $S1P_1$ (EDG1) and LPA_1 (EDG2) phospholipid growth factor receptors, *J. Biol. Chem.* 276 (2001) 49213–49220.
- [31] H. Berman, K. Henrick, H. Nakamura, Announcing the worldwide Protein Data Bank, *Nat. Struct. Biol.* 10 (2003) 980.
- [32] T.C. Pham, R.W. Kriwacki, A.L. Parrill, Peptide design and structural characterization of a GPCR loop mimetic, *Biopolymers* 86 (2007) 298–310.
- [33] MOE, Chemical Computing Group: Montreal, 2003.
- [34] T.A. Halgren, Merck molecular force field. I. Basis form, scope parameterization, and performance of MMFF94*, *J. Comput. Chem.* 17 (5/6) (1996) 490–519.
- [35] G.M. Morris, D.S. Goodsell, R.S. Halliday, R. Huey, W.E. Hart, R.K. Belew, A.J. Olson, Automated docking using a Lamarckian genetic algorithm and an empirical binding free energy function, *J. Comput. Chem.* 19 (1998) 1639–1662.
- [36] E. Jo, M.G. Sanna, P.J. Gonzalez-Cabrera, S. Thangada, G. Tigyi, D.A. Osborne, T. Hla, A.L. Parrill, H. Rosen, $S1P_1$ -selective in vivo-active agonists from high-throughput screening: off-the-shelf chemical probes of receptor interactions, signaling, and fate, *Chem. Biol.* 12 (2005) 703–715.
- [37] J.J. Hale, C.L. Lynch, W. Neway, S.G. Mills, R. Hajdu, C.A. Keohane, M.J. Rosenbach, J.A. Milligan, G.J. Shei, S.A. Parent, G. Chrebet, J. Bergstrom, D. Card, M. Ferrer, P. Hodder, B. Strulovici, H. Rosen, S. Mandala, A rational utilization of high-throughput screening affords selective, orally bioavailable 1-benzyl-3-carboxyazetidine sphingosine-1-phosphate-1 receptor agonists, *J. Med. Chem.* 47 (2004) 6662–6665.
- [38] J.J. Clemens, M.D. Davis, K.R. Lynch, T.L. Macdonald, Synthesis of benzimidazole based analogues of sphingosine-1-phosphate: discovery of potent, subtype-selective $S1P_4$ receptor agonists, *Bioorg. Med. Chem. Lett.* 14 (2004) 4903–4906.
- [39] K.S.C. Reid, P.F. Lindley, J.M. Thornton, Sulfur–aromatic interactions in proteins, *FEBS Lett.* 190 (1985) 209–213.
- [40] H.S. Lim, Y.S. Oh, P.G. Suh, S.K. Chung, Syntheses of sphingosine-1-phosphate stereoisomers and analogues and their interaction with EDG receptors, *Bioorg. Med. Chem. Lett.* 13 (2003) 237–240.
- [41] H.S. Lim, J.J. Park, K. Ko, M.H. Lee, S.K. Chung, Syntheses of sphingosine-1-phosphate analogues and their interaction with EDG/S1P receptors, *Bioorg. Med. Chem. Lett.* 14 (2004) 2499–2503.
- [42] G. Holdsworth, D.A. Osborne, T.T. Pham, J.I. Fells, G. Hutchinson, G. Milligan, A.L. Parrill, A single amino acid determines preference between phospholipids and reveals length restriction for activation of the $S1P_4$ receptor, *BMC Biochem.* 5 (2004) 12.
- [43] M.G. Sanna, J. Liao, E. Jo, C. Alfonso, M.Y. Ahn, M.S. Peterson, B. Webb, S. Lefebvre, J. Chun, N. Gray, H. Rosen, Sphingosine 1-phosphate ($S1P$) receptor subtypes $S1P_1$ and $S1P_3$, respectively,

- regulate lymphocyte recirculation and heart rate, *J. Biol. Chem.* 279 (2004) 13839–13848.
- [44] N. Vaidehi, W.B. Floriano, R. Trabanino, S.E. Hall, P. Freddolino, E.J. Choi, G. Zamanakos, W.A.I. Goddard, Prediction of structure and function of G protein-coupled receptors, *Proc. Natl. Acad. Sci. U.S.A.* 99 (2002) 12622–12627.
- [45] Y. Zhang, M.E. Devries, J. Skolnick, Structure modeling of all identified G protein-coupled receptors in the human genome, *PLoS Comput. Biol.* 2 (2006) e13.
- [46] M.M. Naor, M.D. Walker, J.R. Van Brocklyn, G. Tigyi, A.L. Parrill, Sphingosine 1-phosphate pK(a) and binding constants: intramolecular and intermolecular influences, *J. Mol. Graph. Model.* 26 (2007) 519–528.